Surface Tensions at Elevated Pressure Depend Strongly on Bulk Phase Saturation

Zachary R. Hinton[a], Nicolas J. Alvarez[a,*]

[a]*Drexel University, Department of Chemical and Biological Engineering, Drexel University, Philadelphia, PA 19104*

Abstract

Hypothesis. Understanding interfacial phenomena at elevated pressure is crucial to the design of a variety of processes, modeling important systems, and interpreting interfacial thermodynamics. While many previous studies have offered insight into these areas, current techniques have inherent drawbacks that limit equilibrium measurements.

Experiments. In this work, we adapt the ambient microtensiometer of Alvarez and co-workers into a high pressure microtensiometer (HPMT) capable of experimentally quantifying a wide range of interfacial phenomena at elevated pressures. Particularly, the HPMT uses a microscale spherical interface pinned to the tip of a capillary to directly measure surface tension via the Laplace equation. The stream of microscale bubbles used to pressurize the system ensures quick saturation of the bulk phases prior to conducting measurements. The HPMT is validated by measuring the surface tension of air-water as a function of pressure. We then measure the surface tension of CO_2 vapor and water as a function of pressure, finding lower equilibrium surface tension values than originally reported in the literature.

Findings. This work both introduces further development of a useful experimental technique for probing interfacial phenomena at elevated pressures and demonstrates the importance of establishing bulk equilibrium to measure surface tension. The true equilibrium state of the CO_2-water surface has a lower tension than previously reported. We hypothesize that this discrepancy is likely due to the long diffusion timescales required to ensure saturation of the bulk fluids using traditional tensiometry. Thus we argue that previously reported elevated pressure measurements were performed at non-equilibrium conditions, putting to rest a long standing discrepancy in the literature. Our measurements establish an equilibrium pressure isotherm for the pure CO_2-water surface that will be essential in analyzing surfactant transport at elevated pressures.

Keywords: microtensiometry, elevated pressure, surface tension, carbon dioxide

*Corresponding author
Email address: nja49@drexel.edu (Nicolas J. Alvarez)

1. Introduction

Processes at elevated pressure are increasingly important to a variety of applications. This includes a large number of interfacially driven processes including: cleaning [1, 2, 3, 4, 5], extraction and enhanced oil recovery [6, 7, 8, 9, 10], polymer processing [11, 12, 13, 14, 15], nano-material engineering [16, 17], etc. Understanding the role of pressure on interfacial phenomena is key to predicting process performance and designing novel systems. While this field has been explored by many researchers over the past century, no consistent, generalized framework exists for quantifying and parameterizing the role of pressure on interfacial phenomena for a number of important systems. This means that experimental measurements are required to develop an understanding of how pressure affects interfacial thermodynamics and transport.

Experiments of interfacial phenomena at elevated pressure are arguably limited by cumbersome, time consuming, and difficult to analyze experimental techniques, such as: capillary rise [18, 19, 20], captive drop/bubble [21, 22, 23], and drop shape analysis [24, 25, 26, 27, 28, 29]. The capillary rise and captive bubble techniques are highly dependent on an assumed contact angle, which is not trivial to measure or estimate at elevated pressure. Drop shape analysis is also complicated by the fluid mechanics of drop formation, depletion effects, density effects, and volume dependence [30, 31, 32, 33]. These methods also require an accurate measure of both fluid densities, which are often functions of pressure and phase composition. Additionally, all of these techniques suffer from transport limitations that make it difficult to achieve equilibrium between the bulk phases [34]. The microtensiometer of Alvarez et al. utilizes a microscale interface which promotes measurements of fast adsorption kinetics and reduces the likelihood of depletion effects with a small sample volume [35]. Additionally, the microtensiometer serves as a useful platform for quantifying interfacial phenomena such as interfacial rheology [36, 37], colloidal interactions [38], and transport to spherical interfaces [35, 39, 40]. Thus, the robust nature of the microtensiometer is ideal for systematic experimental measurements of elevated pressure interfacial phenomena.

We argue that equilibrium surface/interfacial tension[1] measurements at elevated pressures are particularly sensitive to bulk phase concentrations. This fact is central to the discrepancies in reported values from the use of the capillary rise and drop shape analysis techniques in the literature [41, 34, 42]. For example, we see from Figure 1 that the equilibrium surface and interfacial tensions between gas, liquid, and supercritical CO_2 and water vary significantly between different studies. More specifically, Tewes and Boury have reported consistently lower $\gamma(P)$ than other researchers, with the largest difference being just before and after the phase transition [41, 43]. The data in Figure 1 at $T \approx 30°C$ represents the largest difference in $\gamma(P)$, however the data of Chun and Wilkinson appear to agree with those of Tewes and Boury at $P \approx 70$ bar, but only for a small range of pressures [20]. At $T \approx 40°C$, nearly all $\gamma(P)$ datasets are in poor agreement. We argue that these discrepancies primarily arise due to poor equilibrium of the bulk phase, which is highly apparatus and user dependent and occurs regardless of the state of CO_2.

In this work, we introduce a high pressure microtensiometer (HPMT) for the purpose of measuring surface tension as a function of pressure. We demonstrate that the HPMT presents several advantages over current instruments making it particularly well suited for experimentally quantifying elevated pressure interfacial phenomena between bulk fluids at equilibrium. We validate the HPMT using the air-water and CO_2-water surfaces, i.e. between the gas and water. Measurements

[1] Note that surface tension is used in this work to refer to a vapor-liquid surface, while interfacial tension refers to a liquid-liquid or supercritical fluid-liquid interface.

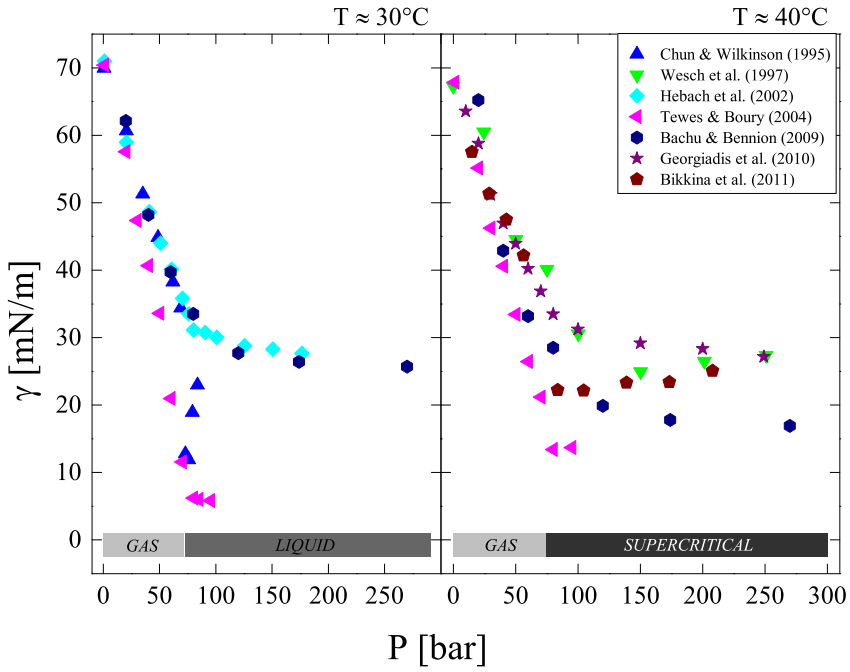

Figure 1: A compilation of data on the equilibrium surface and interfacial tensions, γ, between CO_2 and water as a function of pressure, P [20, 44, 45, 41, 46, 34, 42]. The colored bars show the CO_2 state at the reported pressures, i.e. the relatively constant values are in the dense CO_2 regime. Note that there are considerable differences in reported values.

on the CO_2-water surface are in agreement with previously reported long-time dynamic values. Our results suggest that previous experiments may not have yet achieved bulk thermodynamic equilibrium and therefore measured higher surface tensions. In other words, these results answer a longstanding question in the literature regarding the true surface tension of the CO_2-water system.

2. Experimental Section

2.1. Experimental Setup

A custom experimental microtensiometer setup was built for measurement of surface tension at elevated pressures. The design is a result of further development of the ambient microtensiometer previously reported by Alvarez et al. [35]. A schematic of the high pressure microtensiometer (HPMT) is shown in Figure 2a. The system consists of a main pressure chamber, fluid control and instrumentation, and imaging components. The pressure chamber **(4)** was custom machined from 316 stainless steel, containing threads for all fluid connections and separate thermal fluid paths for temperature control (not employed in this work). The external bulk fluid, in this case water, is introduced using a syringe pump **(5)** which is isolated from pressure using a three-way valve **(6)**. The inner bubble/drop fluid is introduced using a pressurized cylinder with a pressure regulator **(8)**. In this design, the pressurized cylinder is also used to control the desired chamber pressure. Gas from the pressurized cylinder flows through a 2 μm stainless steel filter immediately after the

regulator. The bubble/drop fluid flows from the regulator and selector valve to a custom assembly consisting of a glass micropipette (*World Precision Instruments*, Sarasota, FL) internally fixed to a stainless steel fitting, such that the pressure difference between the inside and outside of the capillary is never large enough to damage the glass. The capillary surface is treated such that the bubble contact line is pinned at the tip of the capillary, as shown in Figure 2b.

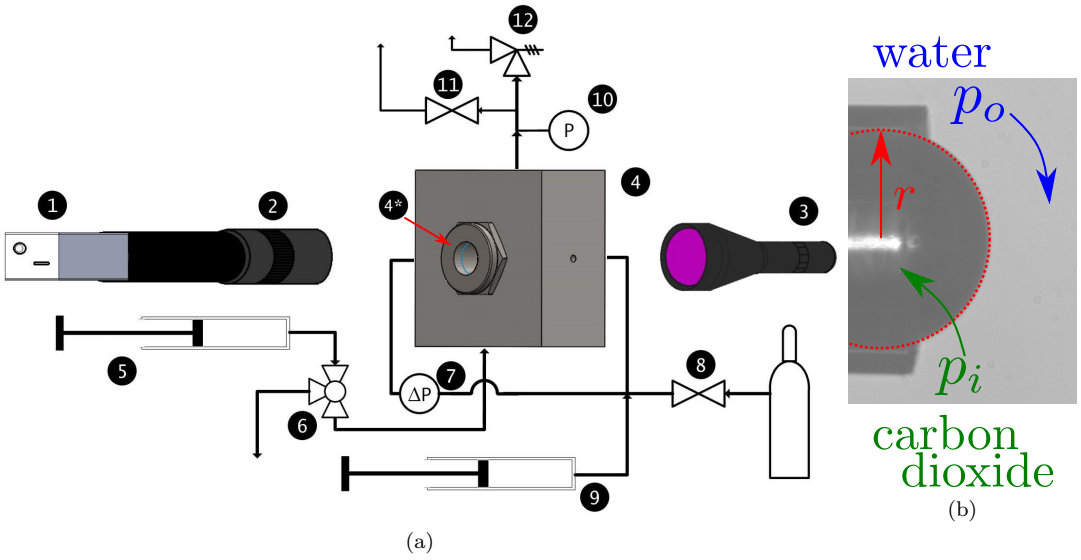

Figure 2: Schematic of the HPMT setup (a) with a typical image of the interface shown in (b).

During operation, the flow of the bubble/drop fluid is controlled by a combination of manipulations via the cylinder regulator and selector valve (*VICI*, Houston, TX) **(8)** with small adjustments using a high pressure syringe pump **(9)** (*Chemyx*, Stafford, TX). The differential pressure between the pressure chamber and the capillary is measured using a differential pressure transducer **(7)** (*Honeywell Sensing and Control*, Golden Valley, MN), with a reported accuracy of ±35 Pa. The differential pressure, $\Delta p = p_i - p_o$, is measured at two horizontal points with no height difference between the points, i.e. no hydrostatic head need be accounted for. The chamber is sealed and vented using a solenoid valve **(11)** with fast response time, and for instrument protection, a pressure relief valve **(12)** is directly attached to the chamber. The chamber pressure is measured using a high pressure gauge transducer **(10)** (*Omega Engineering*, Norwalk, CT), with a reported accuracy of ±0.03% or ∼ 500 Pa.

The imaging components consist of a camera **(1)** (*Point Grey*, Wilsonville, OR) with a nominal frame rate > 100 fps attached to a telecentric, long working distance objective **(2)** with 10× magnification (*Mitutoyo*, Japan) via a lens tube. The optical path travels through two high pressure quartz windows **(4*)** (*Encole*, San Jose, CA) where the tip of the glass pipette is centered in the field of view using a micrometer stage. The image is illuminated by a telecentric illuminator **(3)** (*Edmund Optics*, Barrington, NJ). An example image is shown in Figure 2b.

As with the 'ambient' microtensiometer, the pressure jump across the surface, $\Delta p(t) = p_i - p_o$, and the radius of the surface, $r(t)$, are measured continuously to give surface tension via the Laplace equation, $\gamma(t) = r(t)\Delta p(t)/2$, as described previously [35, 47]. Data acquisition and instrument

control were achieved using a Real-Time Controller with cRIO modules connected to a PC running custom designed LabVIEW software (*National Instruments*, Austin, TX).

2.2. Experimental Procedure

Prior to conducting experiments, pressure instruments were tared and calibrated and the optical system was calibrated following the procedure developed by Hinton and Alvarez [47]. Because of the increased degrees of freedom in the horizontally oriented optical components of the HPMT, the measurement requires a calibration step to account for optical errors due to misalignment [47]. Therefore, the system was first calibrated with DI water at ambient pressure by measuring radius at varied p_i, following the procedure of Hinton and Alvarez. The measured surface tension as a function of measured radius is fit to a linear correction equation, which relates the measured radius, r_m, to the true radius, r, in the form $r = mr_m + b$, as demonstrated in Figure 3. This calibration was then applied to all further radius measurements, such that $r(t) = mr_m(t) + b$. The pressure chamber and attached components were cleaned by flowing several liters of ethanol, ethanol in water, and DI water through the cell until the surface tension at atmospheric pressure was measured to be ~ 72 mN/m and constant for greater than 3000 s.

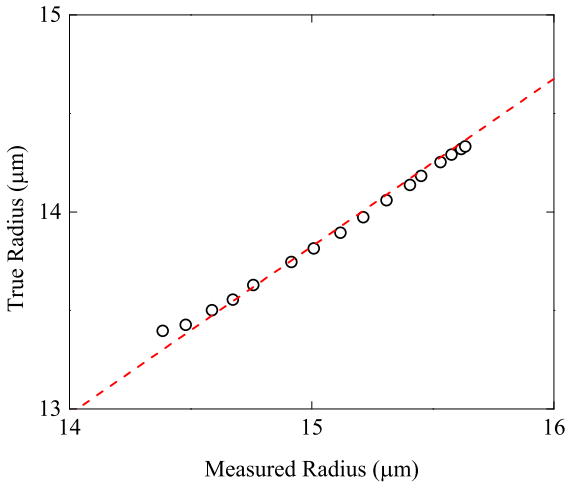

Figure 3: True interfacial radius as a function of the measured radius, as determined using [47]. Points represent calibration measurements and the line represents the calibration curve used in this work.

For $P = 1$ bar absolute, the chamber was open to the atmosphere. For elevated pressures, air or CO_2 gas was injected through the capillary until the pressure in the closed chamber reached the desired setpoint. Once the chamber pressure is at the setpoint value, the selector valve is closed and a fresh interface is pinned to the needle surface. Equilibrium surface tensions, γ, were taken after $\partial\gamma/\partial t$ was negligible, which in all cases was instantaneous. Care was taken to wait until no flow of bubbles was visibly evident before measurements were made. During experiments, no interaction between either the interface or the capillary surface with undissolved droplets was observed. For all measurements, no change in $\gamma(t)$ was observed for $> 10^3$ s, therefore equilibrium γ values were taken as the mean of $\gamma(t)$ over all time points. The reported values represent the average over at least 3 different surfaces, each of which consists of at least 100 points in time. Error is quantified using t-distribution, 95% confidence intervals on the mean.

2.3. Materials

Compressed carbon dioxide and air (research grade) were obtained from *Airgas* (Radnor, PA) and used as received. Fresh deionized water (18.2 $M\Omega{\cdot}cm$) was used for each series of measurements.

3. Results and Discussion

The HPMT is first validated using the air-water surface. Accurate standards for $\gamma(P)$ are not obvious based on the available literature, however air represents an important fluid which is typically used to validate ambient instruments. Furthermore, it is minimally soluble in water and therefore $\gamma(P)$ is less dependent on saturation of the bulk. Figure 4 shows the results of HPMT measurements of air as compared to literature examples for $\gamma(P)$ using nitrogen and oxygen gasses. No actual measurements of $\gamma(P)$ for air have been found in the literature, but from the work of Massoudi and King, it appears that oxygen and nitrogen exhibit identical $\gamma(P)$. While previous work has shown that gas mixtures can cause non-linear dependence of γ as a function of pressure and concentration [48], we expect that air exhibits ideal mixing at the surface, meaning $\gamma_{air} = \gamma_{O_2} = \gamma_{N_2}$. Our results for air are in good agreement with measurements of both O_2 and N_2 within 3%, i.e. ± 1 mN/m. This deviation may be related to temperature, as Massoudi and King report measurements at 25°C while our measurements are performed at 22.5°C. Additionally, further measurements after allowing the instrument to remain at constant pressure for > 12 hr show identical results. These results serve as a validation of the HPMT's ability to accurately measure surface tension at elevated pressure.

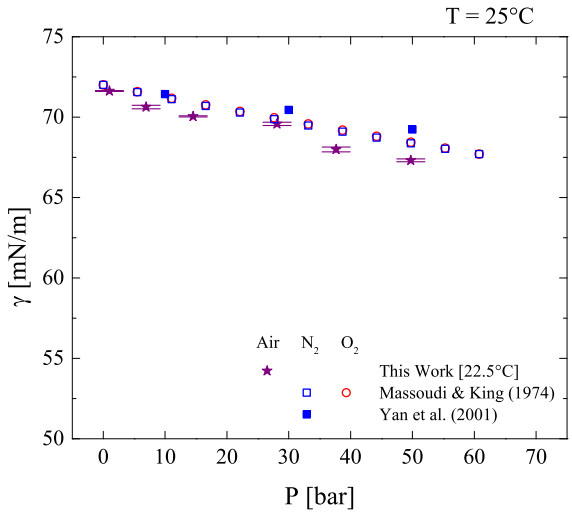

Figure 4: Surface tension of the air-water surface as a function of pressure with comparison to literature values for nitrogen and oxygen, obtained from [19, 49]. Error bars represent 95% confidence intervals on the mean of at least 3 experiments.

We next measure $\gamma(P)$ for the CO_2-water surface. Figure 5 shows the measured values of $\gamma(P)$ compared to literature examples in the same range of pressures. For $P < 40$ bar, our data is in good agreement with previous literature, i.e. within $< 4\%$. For $P > 40$ bar, our measured values are lower than the majority of literature values by up to $\sim 30\%$. However, these values are in line with those obtained by interpolating the data of Tewes and Boury to 25°C [41]. A more detailed comparison

of literature data for $\gamma(P)$ is shown above in Figure 1 for two higher temperatures, where the same trend is observed in Tewes and Boury's dataset, confirming consistently lower measured $\gamma(P)$.

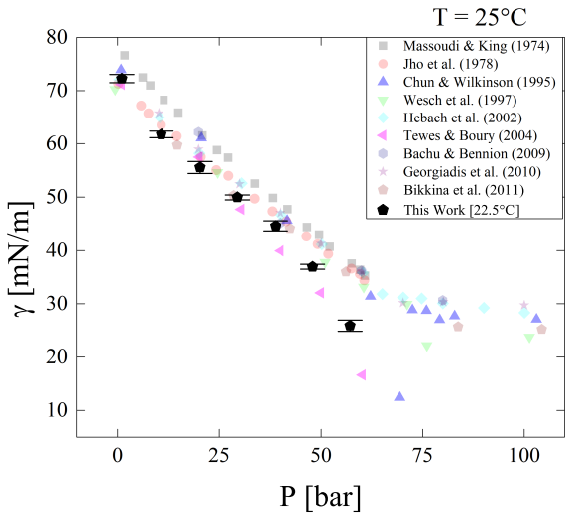

Figure 5: Surface tension of CO_2-water as a function of pressure as measured in this work, black pentagons, and compared to previous reported values in the literature [19, 50, 20, 44, 45, 41, 46, 34, 42]. Error bars represent 95% confidence intervals on the mean of at least 3 experiments. Note that the values of Tewes and Boury are linearly interpolated to 25°C from data at 20 and 30°C.

As discussed in the introduction, equilibrium is a key condition required to correctly measure $\gamma(P)$. The ability to establish equilibrium before measuring the surface tension is one benefit of the high pressure microtensiometer (HPMT). This is achieved, because of the process of pressurizing the HPMT, by flowing bubbles of the gas phase through the bulk fluid. This generates a turbulent flow of microscale bubbles giving a Reynolds number $\approx 2 \times 10^4$, estimated based on the average pressurization rate of 3×10^3 Pa/s, which leads to an average velocity via the ideal gas law and the diameter of the capillary. Fluid properties were estimated for water and CO_2 at 50 bar. This means that convection speeds absorption and diffusion of CO_2 from the bubbles and that the entire bulk volume saturates much faster than if only a single interfacial area is used, which is common practice for previous measurements. Furthermore, previous techniques all have an aqueous drop phase, rather than a gas bubble phase.

Thermodynamic equilibrium between the two phases using the HPMT is confirmed by several observations. First, for multiple vapor phases, the chamber pressure remains constant for at least 2 hr at a fixed initial pressure, therefore we can conclude that the aqueous phase is saturated. This is because the relative volume of head space of gas above the aqueous phase would be significantly depleted if it were to dissolve in the aqueous phase, leading to a noticeable measured pressure reduction. Similarly, no dissolution of the pinned bubble is observed, confirming that saturation is achieved. Finally, several experiments were performed whereby the HPMT was brought to elevated pressure and allowed to remain at that pressure for > 12 hr. Not only was no reduction in pressure observed, repeated measurements of the surface tension yielded the same value.

In a simple, binary system the effect of pressure on surface tension can be derived from equilibrium thermodynamics [54, 55, 56, 57, 58, 59, 60]. At a fixed temperature, these relationships can

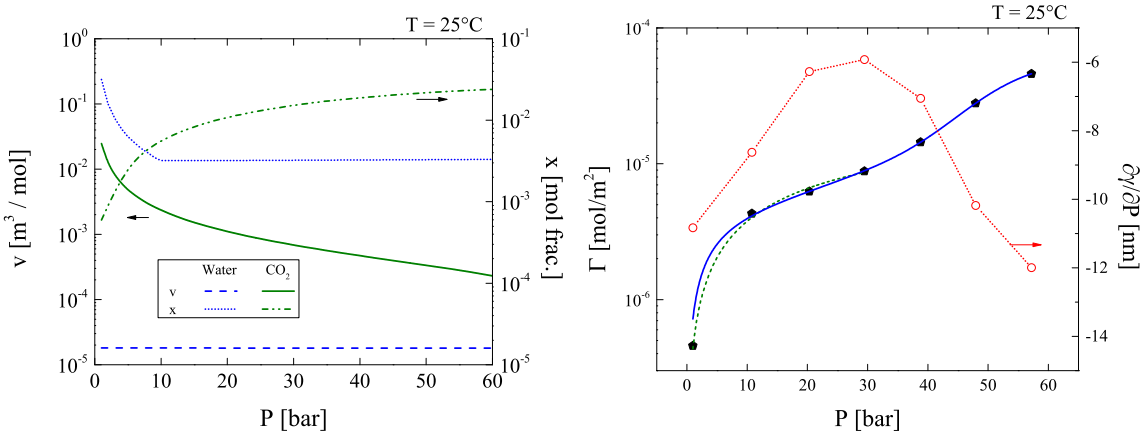

Figure 6: (a) Molar volumes and solubilities for the water-CO_2 system as a function of pressure at $T = 25°C$. Solubilities are for the indicated component when it is the minority constituent of a phase, i.e. the solubility indicated for water and CO_2 represent $x_1^{(II)}$ and $x_2^{(I)}$ in Equation (1), respectively, when CO_2 is chosen as component 2. These values were estimated following Ref. 51 for water and 52 for CO_2. Note that molar volumes correspond to pure fluids and were obtained from Ref. 53. (b) Calculated $\partial\gamma/\partial P$ and Γ as a function of pressure for experiments in the HPMT. The solid and dashed lines represent van der Waals and Langmuir isotherm best fit lines.

be reduced to three main contributions: entropic effects on the molecular density at the surface, surface excess concentration (i.e. adsorption), and changes to bulk phase composition (i.e. saturation). The resulting solution for surface or interfacial tension as a function of pressure, $\gamma(P)$, can be written [60]:

$$\left(\frac{\partial\gamma}{\partial P}\right)_T = -\Gamma_2 \frac{\left(1 - x_2^{(II)}\right) v^{(I)} - \left(1 - x_2^{(I)}\right) v^{(II)}}{x_2^{(I)} - x_2^{(II)}} \tag{1}$$

where x is the mole fraction, v is the molar volume, and Γ is the interfacial excess concentration per unit area. Note that superscripts indicate a property of a given phase and subscripts indicate a property of a given component, e.g. $x_2^{(I)}$ is the mole fraction of component 2 in phase I. Equation (1) is a result of following the Gibbs convention, where the surface is considered two dimensional and located at the point where $\Gamma_1 = 0$. Note that a slightly different solution was derived by Rusanov considering the composition and molar volume of the interfacial phase [59]. For the purpose of this work, Equation (1) is preferable because it has only one parameter characterizing the surface, rather than three.

If we agree that the HPMT measured surface tensions in Figure 5 are at equilibrium, then Equation (1) can be used to estimate the surface concentration of CO_2 as a function of pressure. For this calculation, CO_2 represents component 2 and the vapor phase is denoted by II. Figure 6a shows the relevant thermodynamic parameters in Equation (1) as a function of pressure, using the pure fluid molar volumes as an estimate of the phase volumes. $\partial\gamma/\partial P$ is estimated by the average slope between a given point and its two nearest neighbors, as shown in Figure 6b. Combining these data gives an estimate of the adsorbed concentration of CO_2 at the surface, Γ_2 (simplified to Γ), as shown in Figure 6b. Our data show an order of magnitude increase in CO_2 surface concentration

between 1 and 10 bar, due to a large increase in the solubility of CO_2. A maximum in $\partial\gamma/\partial P$ is observed around 30 bar, where only the molar volume of CO_2 is a strong function of pressure. The decreasing value of $\partial\gamma/\partial P$ beyond this pressure leads to an inflection in Γ at ~ 35 bar, after which the adsorbed concentration is a stronger function of pressure. This is in line with previous works that show good agreement between the density gradient across a surface and its measured surface tension [61].

Interestingly, the surface does not seem to approach a maximum excess surface concentration significantly before the phase transition, suggesting that density more strongly affects the concentration of CO_2 at the surface than solubility. This has implications on the type of isotherm that best describes the adsorption of CO_2 to the surface. For example, if we assume Langmurian adsorption of CO_2, given by:

$$\Gamma_2 = \Gamma_\infty \frac{KP}{1+KP}, \tag{2}$$

where K is the equilibrium constant, and P is the bulk pressure, we find satisfactory agreement at pressures < 30 bar. This suggests that CO_2 may follow ideal adsorption at lower pressures. However, the inflection at $P > 30$ bar resembles type IV multi-layer, e.g. van der Waals adsorption [62], with a generalized isotherm given by

$$\Gamma_2 = \Gamma_\infty \frac{Cy}{1-y} \frac{1 + \left(\frac{ng}{2} - n\right) y^{n-1} - (ng - n + 1)\, y^n + \frac{ng}{2} y^{n+1}}{1 + (C-1)y + \left(\frac{Cg}{2} - C\right) y^n - \frac{Cg}{2} y^{n+1}}, \tag{3}$$

where $y = P/P_0$, P_0 is the vapor pressure, C and g are constants related to the heats of adsorption and evaporation, respectively, and n is the number of adsorbed layers. These equations were fit to the data for Γ using least squares minimization, with best fit lines shown in Figure 6b and parameters and R^2 values given in Table 1. The fact that the van der Waals equation fits well suggests that CO_2 at high pressure leads to complex adsorbed layers. The complexity of the CO_2-water surface is of great importance to interfacial phenomena, such as surface elasticity and surfactant systems where the CO_2 adsorbed layer is expected to effect thermodynamics. For example, this could explain the measured interfacial elasticities reported by Tewes and Boury [41]. In any case, these results and interpretations would be greatly improved via MD simulations of the CO_2-water surface.

Table 1: Pressure adsorption isotherm parameters for the CO_2-water surface.

	Langmuir	**van der Waals**
Γ_∞ (mol/m^2)	2.56×10^{-5}	4.96×10^{-6}
K (1/bar)	1.73×10^{-2}	–
C	–	9.83
n	–	13
P_0 (bar)	–	60
R^2	0.9889	0.9999

3.1. Dynamic Surface Tension

One important characteristic of previous CO_2-water measurements is the observed surface tension dynamics of the clean surface, first reported by Hebach et al. [45]. They observed three distinct regimes in $\gamma(t)$: (i) an initial relaxation due to diffusion of bulk fluid components into the

opposing phase, (ii) a quasi-static state considered to yield the equilibrium surface tension, and (iii) a long time relaxation process caused by 'drop aging'. Before this classification, researchers only attempted to ensure equilibrium between phases [19, 50, 20, 44], however their reported $\gamma(P)$ appears to compare well with the data from interval (ii) reported by other researchers [45, 34]. Tewes and Boury first reported a fourth interval whereby the long time relaxation led to an additional static state after $t > 5 \times 10^4$ s, which they considered the thermodynamic equilibrium surface tension [41, 43]. Figure 7b illustrates the two main types of dynamics reported in the literature [43, 34]. Note that these dynamics are for illustrative purposes and occur at different T and P than measured on the HPMT. While the literature agrees that the initial relaxation and static state represents non-equilibrium transport of CO_2, it is unclear whether the second static state is indeed an equilibrium state or an artifact.

One important observation that results from a quantitative comparison of the dynamic surface/interfacial tensions reported in the literature, is that all data show strong dependencies on the sample volume, setup, and sometimes pressure. For example, some researchers show $\gamma(t)$ with an intermediate plateau of either zero slope[45] or moderately negative slopes [43]. While some experimental conditions in the same work exhibit simple dynamics with long relaxation times[43], others appear to show extremely slow dynamics that are clearly not at equilibrium [42].

In our measurements, no dynamic effects were observed, as shown by examples in Figure 7a. As the dynamics show, no change in surface tension occurs over a period of ~ 1000 s. While this timescale is smaller than the previously reported dynamics, there is no indication of decreasing $\gamma(t)$, which would be expected to begin for $t < 1000$ s. As discussed above, no dissolution of bubbles or changes in the bulk pressure were observed, confirming that the system is at equilibrium for each measured pressure. We therefore conclude that at true equilibrium, no dynamics should be expected for the binary system. Interestingly, we are likely observing the same equilibrium state as measured by Tewes and Boury, without requiring extremely long equilibration times.

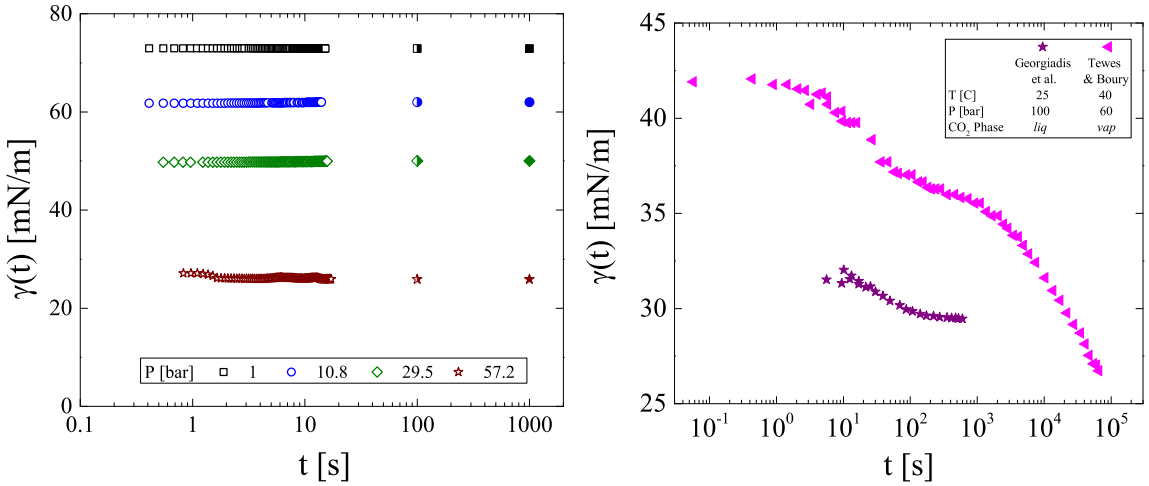

(a) (b)

Figure 7: Dynamic interfacial/surface tension for the CO_2-water interface/surface at selected pressures (a) and from [34, 43] (b). The data points in (a) at $t = 100$ s and $t = 1000$ s represent observed values after continuous recording was stopped.

The first stage relaxation of $\gamma(t)$ has always been attributed to mass transfer leading to saturation of the water phase, i.e. equilibrium [45, 63, 34, 42, 41, 43]. However, a timescale argument can be made to explain that even the long time dynamics represent a path to equilibrium. Take for example an initially pure drop of water (or spherical cap for capillary rise) in contact with pure CO_2 gas. At time equal to zero, the water immediately begins to absorb CO_2 and CO_2 begins to absorb water through the surface. The exchange of CO_2 and water continues until thermodynamic equilibrium is achieved. It is expected that the CO_2 gas will achieve equilibrium before the water droplet (commonly for experiments where excess liquid phase is present). Thus, the timescale required to achieve equilibrium is the diffusion timescale for the drop, which has been shown to be [64]:

$$\tau_{D,s} = \frac{b^2}{D} \tag{4}$$

where b is the drop radius and D is the diffusion coefficient of aqueous CO_2. Thus for most measurement conditions (see Georgiadis et al. [34]), $\tau_{D,s} \approx 10^3$ s [65, 66], which is in line with the reported dynamics or with the time allowed for equilibration prior to measurements. One additional concern has been raised by Hebach et al. suggesting that true equilibrium cannot exist between phases because of the curvature, however this principle seems to only be important on the nanoscale and is inherent to most surface/interfacial tension measurements even at ambient pressures [67].

The secondary relaxation of $\gamma(t)$ ($t > 1000$s) has been attributed to several 'aging effects', such as: corrosion of the capillary, aqueous phase reactions, surface active impurities, or dynamic density changes or inaccuracy due to phase composition [45, 63, 34, 42, 68, 41]. Another effect that has been extensively discussed is the evaporation of water to saturate the CO_2 phase [45, 63], suggesting that the bulk phases were not fully at equilibrium. Furthermore, evaporation is a moot point since most researchers report introducing substantial amounts of water to saturate the vapor phase prior to measuring surface tension. Equation (1) illustrates that $\gamma(P)$ is much less sensitive to the vapor composition than the aqueous composition because $v^{(vap)} \gg v^{(aq)}$.

The operating principle of the HPMT, measurements of the air-water surface, and the absence of dynamics indicate that these effects are unlikely to be responsible for our reported lower equilibrium $\gamma(P)$ values. Tewes and Boury attributed their lower $\gamma(P)$ values to long time aggregation and interfacial reorientation of CO_2-water complexes formed by hydrogen bonding [41]. However, in their studies, this equilibrium state was only achieved after $> 5 \times 10^4$ s, whereas we achieve approximately the same values instantaneously. Interestingly, at the vapor-liquid surface Tewes and Boury showed no appreciable change in the interfacial elasticity, suggesting that the aggregate concentration at the surface would be very small. Furthermore, researchers have not reached a consensus on the presence or stability of such aggregates above room temperature or their mechanism of lowering interfacial tension. If aggregates are responsible for the lower equilibrium $\gamma(P)$, it is unlikely that the kinetics of association would depend on whether water is the drop fluid or the surrounding fluid and would not likely depend on the radius of curvature. Thus the results from the HPMT suggest this explanation may be insufficient at the vapor-liquid surface.

Given that the HPMT promotes saturation conditions at $t = 0$, we argue that previous attempts were measured out-of-equilibrium. In other words, reported dynamic surface tension was tracking the establishment of equilibrium. The timescale arguments of Georgiadis et al.only considered the timescale required to reach saturation of the drop. However, they ignored the fact that the drop was connected to a cylindrical column of water, i.e. the capillary/needle, that also would uptake CO_2. This leads to a nearly infinite reservoir of water that would require saturation.

Diffusion in this domain would follow the timescale: $\tau_{D,c} = \frac{L^2}{D}$, where L is the length-scale of the domain, corresponding to the length of needle, capillary, etc. that is full of water in the system. Although many researchers have noted leaving their fluids in contact for long times to hypothetically equilibrate this domain, the typical timescales for common experimental setups are much longer than reported. For example, for a typical setup $\tau_{D,c} > 6 \times 10^5$ s, or $\tau_{D,c} > 7$ days. Note that some systems include additional contact area between CO_2 and water, however this would only speed diffusion by a maximum factor of 4, if the length-scale is halved.

One argument against the timescale analysis above is that the reported dynamics at the CO_2-water surface are very reproducible within a given setup, meaning that subsequent drops exhibit the same initial relaxation. However, this is unsurprising given that the times required for the system to equilibrate are orders of magnitude larger than the experimental observations reported. In other words, pushing out subsequent drops would only restart the saturation process again from only a slightly closer to equilibrium bulk phase. Our results and arguments are supported in part by modeling efforts. For example, Ravera and coworkers modeled a liquid-liquid system of unsaturated phases [69]. They clearly showed that for these systems $\gamma(t)$ can pass through a quasi-static state at timescales comparable to local drop equilibrium, but a sustained flux leads to a secondary relaxation to equilibrium. Our argument appears to connect the dynamic timescales of Tewes and Boury and equilibrium $\gamma(P)$ measured by the HPMT in the absence of dynamics. It is also thermodynamically consistent with Equation (1), and does not require a discussion of complex interfacial physics. Therefore, we must conclude that previous reports were typically measuring out-of-equilibrium surface tension values.

If our arguments are correct, these results have important implications for future studies and modeling. For one, it means that γ_{eq} requires more than the drop to be at equilibrium. In other words, γ_{eq} is only achieved when global, bulk saturation is established. Although we only demonstrate saturation between CO_2 gas and water, we expect that bulk saturation between liquid or supercritical CO_2 and water would lead to consistent interfacial tension measurements. We note that one major advantage of the HPMT is that bulk saturation is achieved during pressurization of the system. One important implication of ensuring bulk saturation is the study of surfactant transport and equilibrium. More specifically, it would be extremely difficult, almost improbable, to measure dynamic or equilibrium surface tension for surfactant systems if the 'clean' surface itself is evolving in time. The HPMT offers a significant advantage in this regard, which will be the subject of future investigations.

4. Conclusions

Experimental measurements of interfacial phenomena as a function of pressure are critical for design and optimization of a large number of processes. Few thermodynamic theories have been proposed to quantify surface tension as a function of pressure. Furthermore, parameterization and validation of these models requires rigorous experimental quantification. Unfortunately, experimental apparatuses have limited the measurement of such systems because they are often difficult to construct and operate at elevated pressure [45, 34, 42]. In this work we have introduced the high pressure microtensiometer (HPMT). The HPMT provides a robust measurement platform that is ideal for elevated pressure measurements, particularly because density values are made irrelevant, timescales for adsorption are decreased, and equilibrium saturation is ensured prior to measurements.

The HPMT was validated using the air-water surface as a function of pressure. The results confirm that $\gamma(P)$ for air is equal to that of both oxygen and nitrogen. Our measurements of the CO_2-water surface reveal important experimental design considerations when performing elevated pressure interfacial measurements. First, no dynamics are measured in γ, demonstrating the absence of mass transfer, i.e. fluids are saturated before measurement. Second, the equilibrium surface tension of CO_2-water is lower than previously reported, agreeing with the extremely long time steady state values of Tewes and Boury [41, 43]. Note that Tewes and Boury argue that the long time surface tension is due to some dynamic molecular effects at the interface, such as the formation of complexes that are argued to form over time. Our data clearly shows that there are no dynamic molecular changes to the CO_2-water surface when bulk saturation is ensured. As such, it appears that local equilibrium between the outer and drop fluids may not be enough to obtain equilibrium surface tension as a function of pressure. At equilibrium, the calculated surface concentration of CO_2 suggests complex multi-layer interfacial adsorption of CO_2 at elevated pressure. This finding strongly impacts the current understanding of interfacial phenomena as a function of pressure, which will inevitably impact modeling and physical interpretation of similar systems. Particularly the design of extraction [6, 7], colloidal [16, 11], and other interfacial processes [1] at elevated pressures must consider the equilibrium surface/interfacial tension.

Overall, the HPMT represents a versatile experimental platform which allows for consistent measurements of the role of pressure on interfacial phenomena. Its benefits warrant use in all areas of elevated pressure interfacial phenomena. Particularly, the ability to achieve equilibrium between the bulk fluids is crucial to distinguishing between interfacial processes. This is even more important for surfactant systems, where previous measurements were likely measuring dynamics of both CO_2 and surfactant transport, and for dense fluid-fluid systems, where measurements are affected by phase saturation. This has likely led to inaccurate parameters for elevated pressure surfactant systems and hypotheses that likely do not hold in a system truly at equilibrium. Future studies will investigate the dynamic and equilibrium surface tension of surfactants at the CO_2-water surface as a function of elevated pressures. This will undoubtedly lead to more critical design of novel processes and surfactants for elevated pressure [70].

Acknowledgment

This work was supported by the National Science Foundation under grant no. CBET-1847140.

References

[1] S. Banerjee, S. Sutanto, J. M. Kleijn, M. J. E. Van Roosmalen, G. J. Witkamp, M. a. C. Stuart, Colloidal interactions in liquid CO 2 - A dry-cleaning perspective, Adv. Colloid Interface Sci. 175 (2012) 11–24. doi:10.1016/j.cis.2012.03.005.
URL `http://dx.doi.org/10.1016/j.cis.2012.03.005`

[2] M. J. E. Van Roosmalen, G. F. Woerlee, G. J. Witkamp, Amino acid based surfactants for dry-cleaning with high-pressure carbon dioxide, J. Supercrit. Fluids 32 (1-3) (2004) 243–254. doi:10.1016/j.supflu.2004.01.005.

[3] M. J. E. Van Roosmalen, G. F. Woerlee, G. J. Witkamp, Surfactants for particulate soil removal in dry-cleaning with high-pressure carbon dioxide, J. Supercrit. Fluids 30 (1) (2004) 97–109. doi:10.1016/S0896-8446(03)00115-3.

[4] N. M. Lawandy, A. Y. Smuk, Supercritical fluid cleaning of banknotes, Ind. Eng. Chem. Res. 53 (2) (2014) 530–540. doi:10.1021/ie403307y.

[5] J. a. Keagy, Y. Li, P. F. Green, K. P. Johnston, F. Weber, J. T. Rhoad, E. L. Busch, P. J. Wolf, CO2 promotes penetration and removal of aqueous hydrocarbon surfactant cleaning solutions and silylation in low-k dielectrics with 3 nm pores, J. Supercrit. Fluids 42 (3 SPEC. ISS.) (2007) 398–409. doi:10.1016/j.supflu.2007.02.007.

[6] M. Mazzotti, R. Pini, G. Storti, Enhanced coalbed methane recovery, J. Supercrit. Fluids 47 (3) (2009) 619–627. doi:10.1016/j.supflu.2008.08.013.

[7] M. Blunt, F. Fayers, F. M. Orr, Carbon dioxide in enhanced oil recovery, Energy Convers. Manag. 34 (9-11) (1993) 1197–1204. doi:10.1016/0196-8904(93)90069-M.

[8] a. M. F. Palavra, J. P. Coelho, J. G. Barroso, a. P. Rauter, J. M. N. a. Fareleira, a. Mainar, J. S. Urieta, B. P. Nobre, L. Gouveia, R. L. Mendes, J. M. S. Cabral, J. M. Novais, Supercritical carbon dioxide extraction of bioactive compounds from microalgae and volatile oils from aromatic plants, J. Supercrit. Fluids 60 (2011) 21–27. doi:10.1016/j.supflu.2011.04.017.
URL http://dx.doi.org/10.1016/j.supflu.2011.04.017

[9] E. Reverchon, R. Adami, S. Cardea, G. D. Porta, Supercritical fluids processing of polymers for pharmaceutical and medical applications, J. Supercrit. Fluids 47 (3) (2009) 484–492. doi:10.1016/j.supflu.2008.10.001.

[10] J. Porschmann, L. Blasberg, K. Mackenzie, P. Harting, Application of surfactants to the supercritical fluid extraction of nitroaromatic compounds from sediments1, J. Chromatogr. A 816 (2) (1998) 221–232. doi:10.1016/S0021-9673(98)00467-1.
URL http://linkinghub.elsevier.com/retrieve/pii/S0021967398004671

[11] B. Baradie, M. S. Shoichet, Z. Shen, M. a. McHugh, L. Hong, Y. Wang, J. K. Johnson, E. J. Beckman, R. M. Enick, Synthesis and solubility of linear poly(tetrafluoroethylene-co-vinyl acetate) in dense CO 2: Experimental and molecular modeling results, Macromolecules 37 (20) (2004) 7799–7807. doi:10.1021/ma049384u.

[12] J. M. Desimone, E. E. Maury, Y. Z. Menceloglu, J. B. McClain, T. J. Romack, J. R. Combes, Dispersion polymerizations in supercritical carbon dioxide., Science (80-.). 265 (5170) (1994) 356–359. doi:10.1126/science.265.5170.356.

[13] C. Gutiérrez, J. F. Rodríguez, I. Gracia, a. De Lucas, M. T. García, Development of a strategy for the foaming of polystyrene dissolutions in scCO2, J. Supercrit. Fluids 76 (2013) 126–134. doi:10.1016/j.supflu.2013.01.020.
URL http://dx.doi.org/10.1016/j.supflu.2013.01.020

[14] I. Tsivintzelis, A. G. Angelopoulou, C. Panayiotou, Foaming of polymers with supercritical CO2: An experimental and theoretical study, Polymer (Guildf). 48 (20) (2007) 5928–5939. doi:10.1016/j.polymer.2007.08.004.
URL http://dx.doi.org/10.1016/j.polymer.2007.08.004

[15] M. Goto, Chemical recycling of plastics using sub- and supercritical fluids, J. Supercrit. Fluids 47 (3) (2009) 500–507. doi:10.1016/j.supflu.2008.10.011.

[16] F. Cansell, C. Aymonier, Design of functional nanostructured materials using supercritical fluids, J. Supercrit. Fluids 47 (3) (2009) 508–516. doi:10.1016/j.supflu.2008.10.002.

[17] J. D. Holmes, D. M. Lyons, K. J. Ziegler, Supercritical fluid synthesis of metal and semiconductor nanomaterials, Chem. - A Eur. J. 9 (10) (2003) 2144–2150. doi:10.1002/chem.200204521.

[18] C. J. Lynde, Effect of Pressure on Surface Tension, Phys. Rev. 22 (1906) 181–191. arXiv:arXiv:1011.1669v3, doi:10.1017/CBO9781107415324.004.

[19] R. Massoudi, A. D. King, Effect of pressure on the surface tension of water. Adsorption of low molecular weight gases on water at 25 degrees, J. Phys. Chem. 78 (22) (1974) 2262–2266. doi:10.1021/j100615a017.
URL http://dx.doi.org/10.1021/j100615a017

[20] B. S. Chun, G. T. Wilkinson, Interfacial Tension in High-Pressure Carbon Dioxide Mixtures, Ind. Eng. Chem. Res. 34 (12) (1995) 4371–4377. doi:10.1021/ie00039a029.

[21] L. L. Schramm, D. B. Fisher, S. Schiirch, A. Cameron, A captive drop instrument for surface or interfacial tension measurements at elevated tempeartures and pressures, Colloids Surfaces A Physicochem. Eng. Asp. 94 (1995) 145–159.

[22] Y. Liu, M. Mutailipu, L. Jiang, J. Zhao, Y. Song, L. Chen, Interfacial Tension and Contact Angle Measurements for the Evaluation of CO2-Brine Two-Phase Flow Characteristics in Porous Media, Environ. Prog. Sustain. Energy 34 (6) (2015) 1756–1762. doi:10.1002/ep.12160.

[23] V. Mirchi, S. Saraji, L. Goual, M. Piri, Dynamic interfacial tension and wettability of shale in the presence of surfactants at reservoir conditions, Fuel 148 (MAY) (2015) 127–138. doi:10.1016/j.fuel.2015.01.077.
URL http://www.sciencedirect.com/science/article/pii/S0016236115000915

[24] A. S. Michaels, E. A. Hauser, Interfacial tension at elevated pressure and temperature. II Interfacial properties of hydrocarbon-water systems., J. Phys. Chem. 55 (3) (1951) 408–421. doi:10.1021/j150486a008.

[25] P. Chiquet, J. L. Daridon, D. Broseta, S. Thibeau, CO2/water interfacial tensions under pressure and temperature conditions of CO2 geological storage, Energy Convers. Manag. 48 (3) (2007) 736–744. doi:10.1016/j.enconman.2006.09.011.

[26] X. Chen, S. S. Adkins, Q. P. Nguyen, A. W. Sanders, K. P. Johnston, Interfacial tension and the behavior of microemulsions and macroemulsions of water and carbon dioxide with a branched hydrocarbon nonionic surfactant, J. Supercrit. Fluids 55 (2010) 712–723. doi:10.1016/j.supflu.2010.08.019.

[27] A. Firooz, P. Chen, Impact of carbon dioxide on the surface tension of 1-hexanol aqueous solutions, Colloids Surfaces A Physicochem. Eng. Asp. 392 (1) (2011) 355–364. doi:10.1016/j.colsurfa.2011.10.017.
URL http://dx.doi.org/10.1016/j.colsurfa.2011.10.017

[28] K. Yasuda, Y. H. Mori, R. Ohmura, Interfacial tension measurements in water-methane system at temperatures from 278.15 K to 298.15 K and pressures up to 10 MPa, Fluid Phase Equilib. 413 (2016) 170–175. doi:10.1016/j.fluid.2015.10.006.

[29] H. Akiba, R. Ohmura, Surface tension between CO2 gas and tetra-n-butylammonium bromide aqueous solution, J. Chem. Thermodyn. 92 (2016) 72–75. doi:10.1016/j.jct.2015.08.039.
URL http://dx.doi.org/10.1016/j.jct.2015.08.039

[30] C. Yang, Y. Gu, Modeling of the Adsorption Kinetics of Surfactants at the Liquid-Fluid Interface of a Pendant Drop, Langmuir 20 (6) (2004) 2503–2511. doi:10.1021/la0360097.

[31] N. J. Alvarez, L. M. Walker, S. L. Anna, A criterion to assess the impact of confined volumes on surfactant transport to liquid–fluid interfaces, Soft Matter 8 (34) (2012) 8917. doi:10.1039/c2sm25447f.

[32] J. D. Berry, M. J. Neeson, R. R. Dagastine, D. Y. C. Chan, R. F. Tabor, Measurement of surface and interfacial tension using pendant drop tensiometry, J. Colloid Interface Sci. 454 (2015) 226–237. doi:10.1016/j.jcis.2015.05.012.
URL http://dx.doi.org/10.1016/j.jcis.2015.05.012

[33] N. J. Alvarez, L. M. Walker, S. L. Anna, A non-gradient based algorithm for the determination of surface tension from a pendant drop: Application to low Bond number drop shapes, J. Colloid Interface Sci. 333 (2) (2009) 557–562. doi:10.1016/j.jcis.2009.01.074.
URL http://dx.doi.org/10.1016/j.jcis.2009.01.074

[34] A. Georgiadis, G. Maitland, J. P. M. Trusler, A. Bismarck, Interfacial Tension Measurements of the (H2O + CO2) System at Elevated Pressures and Temperatures, J. Chem. Eng. Data 55 (2010) 4168–4175. doi:10.1021/je100198g.
URL http://pubs.acs.org/doi/abs/10.1021/je100198g

[35] N. J. Alvarez, L. M. Walker, S. L. Anna, A microtensiometer to probe the effect of radius of curvature on surfactant transport to a spherical interface, Langmuir 26 (10) (2010) 13310–13319. doi:10.1021/la101870m.

[36] A. P. Kotula, S. L. Anna, Regular perturbation analysis of small amplitude oscillatory dilatation of an interface in a capillary pressure tensiometer, J. Rheol. (N. Y. N. Y). 59 (1) (2015) 85–117. doi:10.1122/1.4902546.

[37] M. S. Manga, T. N. Hunter, O. J. Cayre, D. W. York, M. D. Reichert, S. L. Anna, L. M. Walker, R. A. Williams, S. R. Biggs, Measurements of Submicron Particle Adsorption and Particle Film Elasticity at Oil-Water Interfaces, Langmuir 32 (17) (2016) 4125–4133. doi:10.1021/acs.langmuir.5b04586.

[38] M. D. Reichert, L. M. Walker, Coalescence behavior of oil droplets coated in irreversibly-adsorbed surfactant layers, J. Colloid Interface Sci. 449 (2015) 480–487. doi:10.1016/j.jcis.2015.02.032.
URL http://linkinghub.elsevier.com/retrieve/pii/S0021979715001885

[39] N. J. Alvarez, W. Lee, L. M. Walker, S. L. Anna, The effect of alkane tail length of CiE8 surfactants on transport to the silicone oil-water interface, J. Colloid Interface Sci. 355 (1) (2011) 231–236. doi:10.1016/j.jcis.2010.11.077.
URL http://dx.doi.org/10.1016/j.jcis.2010.11.077

[40] S. M. Kirby, S. L. Anna, L. M. Walker, Sequential Adsorption of an Irreversibly Adsorbed Nonionic Surfactant and an Anionic Surfactant at an Oil/Aqueous Interface, Langmuir (2015) 150402144354001doi:10.1021/la504969v.
URL http://pubs.acs.org/doi/abs/10.1021/la504969v

[41] F. Tewes, F. Boury, Thermodynamic and Dynamic Interfacial Properties of Binary Carbon Dioxide - Water Systems, J. Phys. Chem. B 108 (2004) 2405–2412.

[42] P. K. Bikkina, O. Shoham, R. Uppaluri, Equilibrated interfacial tension data of the CO 2-water system at high pressures and moderate temperatures, J. Chem. Eng. Data 56 (10) (2011) 3725–3733. doi:10.1021/je200302h.

[43] F. Tewes, F. Boury, Formation and rheological properties of the supercritical CO2 - Water pure interface, J. Phys. Chem. B 109 (9) (2005) 3990–3997. doi:10.1021/jp046019w.

[44] A. Wesch, N. Dahmen, K. Ebert, J. Schön, Grenzflächenspannungen, Tropfengrößen und Kontaktwinkel im Zweiphasensystem H2O/CO2 bei Temperaturen von 298 bis 333 K und Drücken bis 30 MPa, Chemie Ing. Tech. 69 (1997) 942–956.

[45] A. Hebach, A. Oberhof, N. Dahmen, A. Kogel, H. Ederer, E. Dinjus, Interfacial tension at elevated pressures-measurements and correlations in the water + carbon dioxide system, J. Chem. Eng. Data 47 (6) (2002) 1540–1546.

[46] S. Bachu, D. B. Bennion, Interfacial tension between CO2, freshwater, and brine in the range of pressure from (2 to 27) MPa, temperature from (20 to 125) ?? C, and water salinity from (0to334 000)mg ?? L-1, J. Chem. Eng. Data 54 (3) (2009) 765–775. doi:10.1021/je800529x.

[47] Z. R. Hinton, N. J. Alvarez, Accounting for optical errors in microtensiometry, J. Colloid Interface Sci. 526 (2018) 392–399. doi:10.1016/j.jcis.2018.04.053.
URL https://doi.org/10.1016/j.jcis.2018.04.053

[48] H. Y. Jennings, G. H. Newman, Effect of temperature and pressure on the interfacial tension of water against methane- normal decane mixtures, Soc Pet. Eng J 11 (2) (1971) 171–175. doi:10.2118/3071-pa.

[49] W. Yan, G.-Y. Zhao, G.-J. Chen, T.-M. Guo, Interfacial Tension of (Methane + Nitrogen) + Water and (Carbon Dioxide + Nitrogen) + Water Systems, J. Chem. Eng. Data 46 (2001) 1544–1548. doi:10.1021/je0101505.

[50] C. Jho, D. Nealon, S. Shogbola, A. D. King Jr., Effect of Pressure on the Surface Tension of Water : Adsorption of Hydrocarbon Gases and Carbon Dioxide on Water at Temperatures between 0 and 50C, J. Colloid Interface Sci. 65 (1) (1978) 141–154.

[51] P. G. Hill, A Unified Fundamental Equation for the Thermodynamic Properties of H2O, J. Phys. Chem. Ref. Data 19 (5) (1990).

[52] L. W. Diamond, N. N. Akinfiev, Solubility of CO2in water from -1.5 to 100C and from 0.1 to 100 MPa: Evaluation of literature data and thermodynamic modelling, Fluid Phase Equilib. 208 (1-2) (2003) 265–290. arXiv:arXiv:1011.1669v3, doi:10.1016/S0378-3812(03)00041-4.

[53] E. W. Lemmon, M. O. McLinden, D. G. Friend, Thermophysical Properties of Fluid Systems, in: P. J. Linstrom, W. G. Mallard (Eds.), NIST Chem. WebBook, NIST Stand. Ref. Database Number 69, National Institute of Standards and Technology, Gaithersburg MD, 20899. doi:10.18434/T4D303.

[54] R. S. Hansen, Thermodynamics of Interfaces Between Condensed Phases, J. Phys. Chem. 66 (5) (1962) 410–415.

[55] J. Eriksson, On the Thermodynamic Theory for the Effect of Pressure on Surface Tension, Acta Chem. Scand. 16 (1962) 2199–2211.

[56] K. Motomura, H. Iyota, M. Aratono, M. Yamanaka, R. Matuura, Thermodynamic consideration of the pressure dependence of interfacial tension, J. Colloid Interface Sci. 93 (1) (1983) 264–269. doi:10.1016/0021-9797(83)90404-6.

[57] G. N. Lewis, M. Randall, Thermodynamics and the Free Energy of Chemical Substances, 1st Edition, McGraw-Hill, New York, 1923.

[58] L. A. Turkevich, J. A. Mann, Pressure Dependence of The Interfacial Tension between Fluid Phases. 1. Formalism and Application to Simple Fluids, Langmuir 6 (2) (1990) 445–456. doi:10.1021/la00092a027.

[59] A. I. Rusanov, V. A. Prokhorov, Interfacial Tensiometry, Elsevier, Amsterdam, 1996. doi:10.1016/S1383-7303(96)80031-7.

[60] M. Kahlweit, On the Effect of Temperature and Pressure on the Interfacial Tension Between Two Liquid Phases, Berichte der Bunsengesellschaft für Phys. Chemie 74 (7) (1970) 636.

[61] A. Georgiadis, F. Llovell, A. Bismarck, F. J. Blas, A. Galindo, G. C. Maitland, J. Trusler, G. Jackson, Interfacial tension measurements and modelling of (carbon dioxide+n-alkane) and (carbon dioxide+water) binary mixtures at elevated pressures and temperatures, J. Supercrit. Fluids 55 (2010) 743–754. doi:10.1016/j.supflu.2010.09.028.

[62] S. Brunauer, L. S. Deming, W. E. Deming, E. Teller, On a theory of the van der waals adsorption of gases, JACS 62 (7) (1940) 1723–1732, publisher: American Chemical Society. doi:10.1021/ja01864a025.

[63] B. Kvamme, T. Kuznetsova, A. Hebach, A. Oberhof, E. Lunde, Measurements and modelling of interfacial tension for water+carbon dioxide systems at elevated pressures, Comput. Mater. Sci. 38 (3) (2007) 506–513. doi:10.1016/j.commatsci.2006.01.020.

[64] N. J. Alvarez, L. M. Walker, S. L. Anna, Diffusion-limited adsorption to a spherical geometry: The impact of curvature and competitive time scales, Phys. Rev. E - Stat. Nonlinear, Soft Matter Phys. 82 (1) (2010) 1–8. doi:10.1103/PhysRevE.82.011604.

[65] S. P. Cadogan, G. C. Maitland, J. P. Trusler, Diffusion coefficients of CO2 and N2 in water at temperatures between 298.15 K and 423.15 K at pressures up to 45 MPa, J. Chem. Eng. Data 59 (2) (2014) 519–525. doi:10.1021/je401008s.

[66] D. Yang, P. Tontiwachwuthikul, Y. Gu, Dynamic interfacial tension method for measuring gas diffusion coefficient and interface mass transfer coefficient in a liquid, Ind. Eng. Chem. Res. 45 (14) (2006) 4999–5008. doi:10.1021/ie060047e.

[67] N. D. Lisgarten, J. R. Sambles, L. M. Skinner, Vapour pressure over curved surfaces-the Kelvin equation, Contemp. Phys. 12 (6) (1971) 575–593. doi:10.1080/00107517108205661.

[68] C. Chalbaud, M. Robin, J. M. Lombard, F. Martin, P. Egermann, H. Bertin, Interfacial tension measurements and wettability evaluation for geological CO2 storage, Adv. Water Resour. 32 (1) (2009) 98–109. doi:10.1016/j.advwatres.2008.10.012.
URL http://dx.doi.org/10.1016/j.advwatres.2008.10.012

[69] F. Ravera, M. Ferrari, L. Liggieri, Adsorption and partitioning of surfactants in liquid-liquid systems, Adv. Colloid Interface Sci. 88 (1-2) (2000) 129–177. doi:10.1016/S0001-8686(00)00043-9.

[70] J. Eastoe, S. Gold, S. Rogers, P. Wyatt, D. C. Steytler, A. Gurgel, R. K. Heenan, X. Fan, E. J. Beckman, R. M. Enick, Designed CO2-philes stabilize water-in-carbon dioxide microemulsions, Angew. Chemie - Int. Ed. 45 (22) (2006) 3675–3677. doi:10.1002/anie.200600397.